Electrocatalysis

DOI: 10.1002/anie.201402311

In Situ Observation of Surface Species on Iridium Oxide Nanoparticles during the Oxygen Evolution Reaction**

*Hernan G. Sanchez Casalongue, May Ling Ng, Sarp Kaya, Daniel Friebel, Hirohito Ogasawara, and Anders Nilsson**

Abstract: *An iridium oxide nanoparticle electrocatalyst under oxygen evolution reaction conditions was probed in situ by ambient-pressure X-ray photoelectron spectroscopy. Under OER conditions, iridium undergoes a change in oxidation state from Ir^{IV} to Ir^{V} that takes place predominantly at the surface of the catalyst. The chemical change in iridium is coupled to a decrease in surface hydroxide, providing experimental evidence which strongly suggests that the oxygen evolution reaction on iridium oxide occurs through an OOH-mediated deprotonation mechanism.*

One of the crucial factors limiting efficient photo-induced water elctrocatalysis is the high overpotential required for the oxygen evolution reaction (OER).[1,2] Of the many materials that can catalyze the OER, iridium(IV) oxide has been shown to have high reactivity and excellent stability in both acidic and basic conditions, in particular being unique as an OER catalyst in acid.[3–6] Nonetheless, the complexity of the electrochemical process still presents many open questions about how this system operates.

First we need to understand the surface speciation of the catalyst under operating conditions. Competing suggestions exist about the chemical nature of iridium(IV) oxide surfaces, ranging from IrO_2,[6,7] to $Ir(OH)_4$,[8] to mixtures of the two.[9] Previous theoretical[10,11] and experimental[9,11–14] efforts are also contradictory on the oxidation state of iridium during the OER process: Some hypotheses involve an Ir^{V} intermediate,[13,14] with a subset of them proposing the OER through a hydroperoxide mechanism,[11,12] while others[9,10] involve the deprotonation of two adjacent hydroxide groups on the same iridium site, resulting in an Ir^{VI} intermediate. Furthermore, the mechanism might change with the pH value of the medium.[13,14] Second, it is essential to discern whether the catalytic process changes the chemical nature of the oxide only in the surface region or also in the bulk. Attempts to address these open questions have been made using many spectroscopic techniques that have provided a wealth of in situ information,[13,14] yet the answers provided have not been fully satisfactory owing to difficulties of simultaneously performing direct, surface-sensitive measurements while electrochemically evolving oxygen.

Herein, we report on the use of synchrotron-radiation-based ambient-pressure photoelectron spectroscopy,[15,16] together with a novel electrochemical cell, to provide operando measurements of the chemical speciation of the iridium oxide surface during OER. We observe that, upon exposure to water, the catalyst surface shows clear signs of partial hydroxylation. We also show that, when the catalyst is evolving oxygen, there is a decrease in surface hydroxide species concurrent with the appearance of Ir^{V}, which indicates that the oxygen evolution reaction occurs on a single iridium site that could favor an OOH intermediate route. Furthermore, by tuning the photon energy of the X-rays, we are capable of probing different depths of the catalyst and determine that these reaction-induced changes are confined to the surface of the catalyst.

Building on previous operando electrochemical APXPS studies,[17,18] the experimental setup consisted of a polymer electrolyte membrane (PEM) electrochemical cell designed to work compatibly with APXPS (Supporting Information: Figure S1). The working electrode side of the membrane was coated with iridium(IV) oxide nanoparticles and the counter electrode, where hydrogen evolves, with platinum nanoparticles (Supporting Information: Experimental Section and Figure S2). The assembled cell was introduced to the APXPS system and hydrated with a pressure of 10 Torr of water, at which point electrochemical characteristics were measured, whereby the onset of OER at the working electrode was observed at an applied voltage of around 1.6 V (see the Supporting Information: Figure S3 for a voltammogram under these experimental conditions).

Figure 1 a shows the Ir 4f spectra of the electrode surface probed with an incident photon energy of 390 eV under a water vapor pressure of 10 Torr at open circuit voltage (OCV, blue) and at an OER operating voltage of 1.75 V (red). As voltage is applied, an increase in intensity is observed at the higher binding energy (BE) regions of both the Ir $4f_{5/2}$ and Ir $4f_{7/2}$ components, as shown in the difference spectrum

[*] H. G. Sanchez Casalongue, Dr. S. Kaya, Dr. D. Friebel, Dr. A. Nilsson
Joint Center for Artificial Photosynthesis (JCAP) Energy Innovation Hub, LBNL
1 Cyclotron Road, MS 976-JCAP, Berkeley, CA 94720 (USA)
E-mail: nilsson@slac.stanford.edu
Dr. M. L. Ng, Dr. H. Ogasawara
SLAC National Accelerator Laboratory
2575 Sand Hill Rd, Menlo Park, CA 94025 (USA)

[**] This material is based upon work performed by the Joint Center for Artificial Photosynthesis, a DOE Energy Innovation Hub, supported through the Office of Science of the U.S. Department of Energy under award no. DE-SC0004993. H.O. gratefully acknowledges the support from Precursory Research for Embryonic Science and Technology (PRESTO) Japan Science and Technology Agency (JST). Portions of this research were carried out at the Stanford Synchrotron Radiation Lightsource (SSRL), a division of SLAC National Accelerator Laboratory and an Office of Science user facility operated by Stanford University for the U.S. Department of Energy.

Supporting information for this article is available on the WWW under http://dx.doi.org/10.1002/anie.201402311.

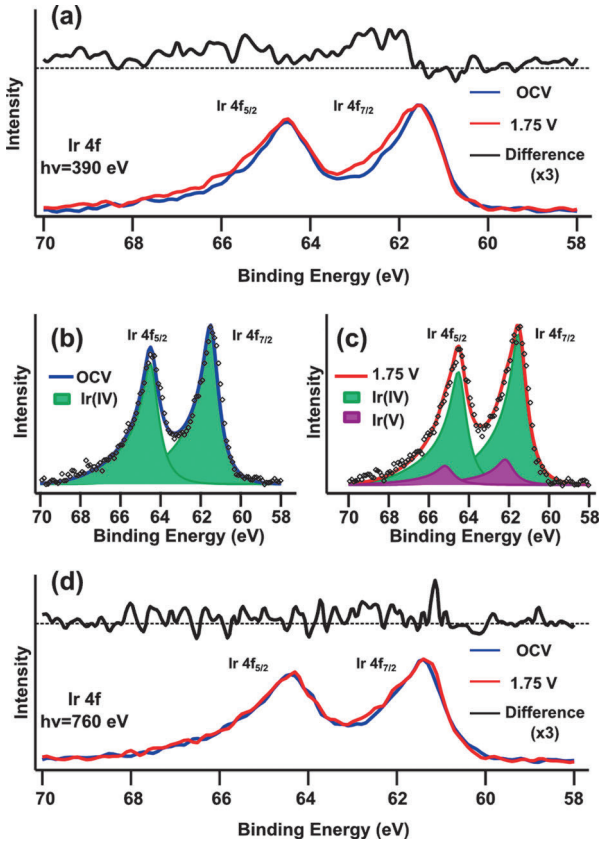

Figure 1. Ir 4f XPS spectra of iridium(IV) oxide nanoparticles under 10 Torr of water. a) Ir 4f signal at open circuit voltage (blue) and during the oxygen evolution reaction (red) collected with an incident photon energy of 390 eV. The black line above corresponds to the difference spectrum. b) Curve-fitted Ir 4f XPS spectrum under open circuit conditions, where the green components corresponds to Ir^{IV}. c) Curve-fitted Ir 4f XPS spectrum under oxygen evolution conditions. The green and purple components correspond to Ir^{IV} and Ir^{V}, respectively. d) Ir 4f signal measured at open circuit voltage (blue) and during oxygen evolution (red) conditions collected with an incident photon energy of 760 eV. The black line above corresponds to the difference spectrum.

(black). This difference is accounted for by two distinctive features at BEs of 62.2 and 65.2 eV, which we attribute to the Ir $4f_{5/2}$ and Ir $4f_{7/2}$ components of iridium atoms that have undergone chemical changes under reaction conditions. This change in the Ir 4f spectra appears solely under oxygen evolving conditions and shows electrochemical reversibility (Supporting Information: Figure S4). No change is observed upon humidification or prolonged acquisition times. Figure 1a is curve-fitted in Figure 1b and c (Supporting Information: Experimental Section). When no current is applied, the open circuit voltage remains under 100 mV and the iridium spectra can be fitted with a single set of components at 61.5 and 64.5 eV (green), in agreement with reported BE values for Ir^{IV}.[7] This single set of components also rules out contributions from metallic iridium, Ir^0, with a reported BE of 60.9 eV.[9] Using the fitting parameters obtained from OCV conditions, it was not possible to recreate the line shape of the spectra under OER conditions, shown in Figure 1c, unless a second set of higher BE components was added into the fit at 62.2 and 65.2 eV (purple). Therefore, both the fit and the difference spectrum support the hypothesis of two distinct iridium oxidation states being present on the catalyst under reaction conditions.

A chemical shift in the XPS BE towards higher values corresponds to an increase in the oxidation state, as observed in previous work[8,9] and well-known for metals and oxides.[19] Considering that platinum and iridium are neighboring elements in the periodic table, we can compare the current results with similar spectral changes in platinum and platinum oxides:[20] For a Pt(111) surface, the BE shift between Pt^0 and Pt^{II} is 0.7 eV, while the shift between Pt^{II} and Pt^{IV} is 2.5 eV, suggesting larger BE shifts for higher oxidation state transitions. This trend is corroborated by molybdenum and tungsten oxides, with BE shifts of 4 and 4.3 eV between the IV and VI oxidation states,[21] and by iridium oxide itself, with a reported BE shift of 1.4 eV between Ir^{IV} and Ir^{VI}.[8] Based on the difference spectra from Figure 1a and the fit from Figure 1c, the new iridium chemical state has a BE 0.7 eV higher than the Ir^{IV} component, which indicates an oxidation state higher than IV but lower than VI. This suggests that the new iridium feature corresponds to an apparent oxidation number of only one unit higher, that is, Ir^{V}, under OER conditions. This finding is in line with previous bulk-sensitive findings only observed in basic pH conditions,[13,14] suggesting the universality of the mechanism. The relative ratios of the components of Figure 1c indicate that 14.6% of the Ir^{IV} within the probing depth (ca. 0.7 nm) is transformed into Ir^{V} under reaction conditions, which suggests that only a fraction of the surface iridium atoms have been transformed during OER.

Along with chemical speciation, XPS/APXPS allows for surface and bulk contributions to be differentiated through varying the probing depth. Figure 1d shows the Ir 4f spectra of the electrode surface with (red) and without (blue) applied voltage at a photon energy of 760 eV. The increase in kinetic energy of the emitted photoelectrons from 325 eV to 700 eV corresponds to an almost doubling of the photoelectron inelastic mean free path, from approximately 0.7 nm to 1.1 nm (Calculated, see Supporting Information: Experimental Section). The difference spectrum shown in Figure 1d (black) still indicates the growth of a higher binding energy feature, but the change is more subtle. Therefore, we propose that the growth of iridium(V) is limited to the top surface layer of the catalyst, explaining why it could not be observed by bulk sensitive techniques.[13,14] Furthermore, this finding indicates that the transformation of Ir^{IV} into Ir^{V} plays a much larger role than the 14.6% of the area in Figure 1c would at first indicate: If we were to restrict all the iridium changes to the top layer of the iridium, the Ir^{V} could represent as much as one third of the surface iridium atoms.

Figure 2a shows the O 1s spectra of the iridium oxide nanoparticle surface, probed with a photon energy of 760 eV for a kinetic energy of 225 eV, under vacuum (green), under 10 Torr of water at OCV (blue), and under both 10 Torr of water and 1.75 V applied voltage (red). The two difference spectra (black) reveal that there are spectral changes as the surface is taken from vacuum to OCV and to OER conditions.

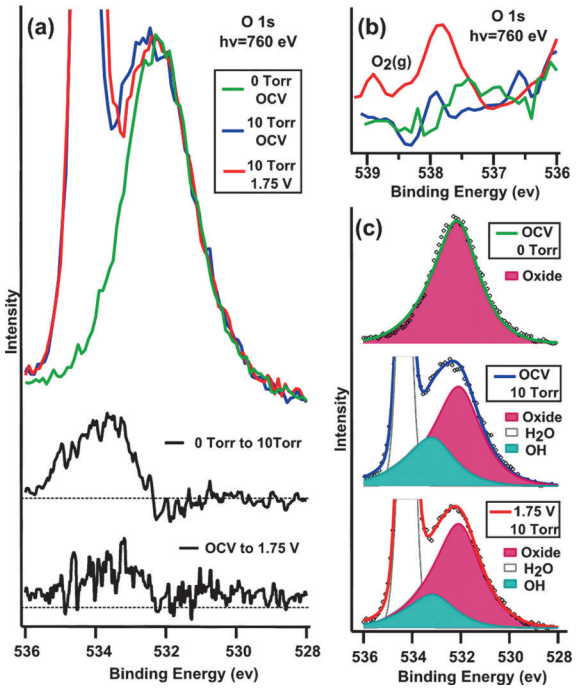

Figure 2. O 1s spectra of iridium oxide nanoparticles collected with an incident photon energy of 760 eV. a) O 1s signal measured under vacuum (green) and under 10 Torr water pressure at open circuit voltage (blue) and during oxygen evolution reaction (red). The black lines below correspond to the difference spectra. b) Higher binding energy region of the O 1s XPS spectra shown in (a). The new component corresponds to gas-phase oxygen being evolved from the catalyst. c) Curve fitted O 1s XPS spectra under vacuum (green), open circuit voltage (blue) and oxygen evolution conditions (red). The gray, teal, and magenta components correspond to water, hydroxide, and oxide components, respectively.

There is also another spectral feature at much higher binding energy, shown at 537.8 eV in Figure 2b, which appears only during OER conditions. This peak corresponds to gas-phase oxygen,[17,22,23] confirming the electrochemical formation of oxygen during the XPS measurements.

The spectra shown in Figure 2a are curve-fitted in Figure 2c. In the OCV and OER O 1s spectra, the intensity of the water gas phase and liquid peak (BE = 534.3 eV) has been truncated to better highlight the relative changes in the surface species. We can differentiate three separate oxygen-containing species through their distinctive binding energies: The first peak, at 532.1 eV (magenta) and the only component of the pristine sample, corresponds to the O^{2-} anions of surface oxides with their oxygen atoms being the most screened owing to the bonding with iridium. Second, we observe OH groups on the surface at a BE of 533.2 eV (teal), consistent with the work in Refs [8,9]. The last species at 534.3 eV (gray) corresponds to water, with signals from adsorbed water and bulk electrolyte overlapping with the gas-phase component, which appears at a lower BE than other works[24–26] owing to the applied voltage.[17] OOH was not included in the fit, as its two characteristic features, 1 and 2.5 eV higher BE than OH,[17,27] would overlap with and be masked by the much larger water component. Although our observed BE values are slightly higher than observed previously,[8] which is most likely due to challenges with the absolute BE calibration (Supporting Information: Experimental Section), the energy separation between species is consistent with previous work,[24,25,28] with the strongly bonded oxides having the lowest BE and the loosely associated water molecules the highest BE. We observe that, as water is introduced and the iridium nanoparticles reach open circuit conditions, part of their surface is covered by adsorbed hydroxide, resulting in a 1:2 hydroxide to oxide ratio (by area). As the Ir 4f signal did not change upon humidification, this means that oxygen atoms are partially transformed to surface hydroxide without changing the oxidation state of iridium. When the system is taken to OER conditions, the ratio of the areas decreases to 1:3, corresponding to a reduction in the amount of adsorbed hydroxide present on the surface. These changes are consistent with previous theoretical works,[11] which postulate that surface hydroxide will be stable on iridium oxide at potentials below 1.5 V vs. RHE, above which the O-containing species become more stable and the surface will be able to undergo the deprotonation step that triggers the oxygen evolution reaction.

In conclusion, our results provide three key findings that will add to the fundamental understanding of the oxygen evolution reaction on iridium oxide nanoparticles: First, we show that iridium oxide nanoparticles in contact with water exhibit a mixed surface composition, with both oxide and hydroxide species coexisting at the same time. Second, we can confirm that the oxygen evolution reaction takes place through a deprotonation mechanism[9] in which hydroxide is converted into oxide on the catalyst surface. Finally, we identify that, as this conversion takes place, there is a potential-dependent change in the oxidation number of iridium from Ir^{IV} to Ir^{V}, showing that Ir^{V} plays an essential role in the OER. However, there seems to be a pH dependence in the depth distribution, as it is detected with in-situ work in base,[13,14] for our results show that the changes in iridium only take place at the top surface layers, explaining why it had not been previously observed by bulk-sensitive techniques under acidic conditions.[13,14] One theory that agrees well with our observation of Ir^{V} proposes the OER mechanism through an OOH intermediate, where the Ir^{V} becomes the energy sink in the reaction since a higher free energy change is required to form the OOH, in agreement with the study by Rossmeisl et al.[11] These results show the versatility of APXPS electrochemistry, and we believe this new technique will open the door to unprecedented fundamental understanding of reaction mechanisms for all electrochemical processes relevant for solar to fuel conversion.

Received: February 11, 2014
Revised: March 27, 2014
Published online: May 28, 2014

Keywords: electrochemistry · iridium oxide · heterogeneous catalysis · oxygen evolution reaction · X-ray photoelectron spectroscopy

[1] J. McKone, N. Lewis, B. Gray, *Chem. Mater.* **2014**, *26*, 407—414.
[2] B. Pinaud, J. Benck, L. Seitz, A. Forman, Z. Chen, T. Deutsch, B. James, K. Baum, G. Baum, S. Ardo, H. Wang, E. Millere, T. F. Jaramillo, *Energy Environ. Sci.* **2013**, *6*, 1983 – 2002.
[3] C. McCrory, S. Jung, J. Peters, T. F. Jaramillo, *J. Am. Chem. Soc.* **2013**, *135*, 16977 – 16987.
[4] Th. Pauporté, F. Andolfatto, R. Durand, *Electrochim. Acta* **1999**, *45*, 431 – 439.
[5] P. Steegstra, E. Ahlberg, *J. Electroanal. Chem.* **2012**, *685*, 1 – 7.
[6] M. Yagi, E. Tomita, T. Kuwabara, *J. Electroanal. Chem.* **2005**, *579*, 83 – 88.
[7] M. Bozack, *Surf. Sci. Spectra* **1993**, *2*, 123.
[8] J. Augustynski, M. Koudelka, J. Sanchez, *J. Electroanal. Chem. Interfacial Electrochem.* **1984**, *160*, 233 – 248.
[9] R. Kötz, H. Neff, S. Stucki, *J. Electrochem. Soc.* **1984**, *131*, 72 – 77.
[10] M. Lyons, L. Burke, *Phys. Chem. Chem. Phys.* **2011**, *13*, 5314 – 5335.
[11] J. Rossmeisl, Z.-W. Qu, H. Zhu, G.-J Kroes, J. Nørskov, *J. Electroanal. Chem.* **2007**, *607*, 83 – 89.
[12] P. Steegstra, E. Ahlberg, *Electrochim. Acta* **2012**, *76*, 26 – 33.
[13] R. Hillman, M. Skopek, S. Gurman, *Phys. Chem. Chem. Phys.* **2011**, *13*, 5252 – 5263.
[14] Y. Mo, I. Stefan, W.-B. Cai, J. Dong, P. Carey, D. A. Scherson, *J. Phys. Chem. B* **2002**, *106*, 3681 – 3686.
[15] S. Kaya, H. Ogasawara, L.-A. Näslund, J.-O. Forsell, H. Sanchez Casalongue, D. Miller, A. Nilsson, *Catal. Today* **2013**, *205*, 101 – 105.
[16] M. Salmeron, R. Schlögl, *Surf. Sci. Rep.* **2008**, *63*, 169 – 199.
[17] H. Sanchez Casalongue, S. Kaya, V. Viswanathan, D. Miller, D. Friebel, H. Hansen, J. Nørskov, A. Nilsson, H. Ogasawara, *Nat. Commun.* **2013**, *4*, 2817.
[18] R. Arrigo, M. Hävecker, M. E. Schuster, C Ranjan, E. Stotz, A. Knop-Gericke, R. Schlögl, *Angew. Chem.* **2013**, *125*, 11874 – 11879; *Angew. Chem. Int. Ed.* **2013**, *52*, 11660 – 11664.
[19] S. Hufner, *Photoelectron spectroscopy: Principles and applications*, 3rd ed., Springer, Heidelberg, **2003**.
[20] D. Miller, H. Sanchez Casalongue, H. Bluhm, H. Ogasawara, A. Nilsson, S. Kaya, *Phys. Rev. Lett.* **2011**, *107*, 195502.
[21] D. Sarma, C. Rao, *J. Electron Spectrosc. Relat. Phenom.* **1980**, *20*, 25 – 45.
[22] H. Bluhm, M. Hävecker, A. Knop-Gericke, E. Kleimenov, R. Schlögl, *J. Phys. Chem. B* **2004**, *108*, 14340 – 14347.
[23] S. Blomberg, M. J. Hoffmann, J. Gustafson, N. M. Martin, V. R. Fernandes, A. Borg, Z. Liu, R. Chang, S. Matera, K. Reuter, E. Lundgren, *Phys. Rev. Lett.* **2013**, *110*, 117601.
[24] J. Newberg, D. Starr, S. Yamamoto, S. Kaya, T. Kendelewicz, E. Mysak, S. Porsgaard, M. Salmeron, G. E. Brown, A. Nilsson, H. Bluhm, *Surf. Sci.* **2011**, *605*, 89 – 94.
[25] S. Yamamoto, T. Kendelewicz, J. Newberg, G. Ketteler, D. Starr, E. Mysak, K. Andersson, H. Ogasawara, H. Bluhm, M. Salmeron, G. E. Brown, A. Nilsson, *J. Phys. Chem. C* **2010**, *114*, 2256 – 2266.
[26] S. Sunde, I. Lervik, M. Tsypkin, L. Owe, *Electrochim. Acta* **2010**, *55*, 7751 – 7760.
[27] J. MacNaughton, L.-A. Näslund, T. Anniyev, H. Ogasawara, A. Nilsson, *Phys. Chem. Chem. Phys.* **2010**, *12*, 5712 – 5716.
[28] T. Kendelewicz, S. Kaya, J. T. Newberg, H. Bluhm, N. Mulakaluri, W. Moritz, M. Scheffler, A. Nilsson, R. Pentcheva, G. E. Brown, *J. Phys. Chem. C* **2013**, *117*, 2719 – 2733.
[29] T. Reier, M. Oezaslan, P. Strasser, *ACS Catal.* **2012**, *2*, 1765 – 1772.
[30] D. Briggs, M. P. Seah, *Practical Surface Analysis: Auger and X-ray photoelectron spectroscopy*, Wiley, New York, **1990**.

